Evolution of internal stresses in the plain ferritic steel studied by neutron diffraction *in situ* upon tensile straining

2009 J. Phys.: Condens. Matter 21 095407

(http://iopscience.iop.org/0953-8984/21/9/095407)

IOP PUBLISHING JOURNAL OF PHYSICS: CONDENSED MATTER

J. Phys.: Condens. Matter **21** (2009) 095407 (7pp) doi:10.1088/0953-8984/21/9/095407

Evolution of internal stresses in the plain ferritic steel studied by neutron diffraction *in situ* upon tensile straining

V Davydov[1,2], P Lukáš[1], P Strunz[1] and R Kužel[3]

[1] Nuclear Physics Institute, 250 68 Řež, Czech Republic
[2] Faculty of Nuclear Sciences and Physical Engineering, Czech Technical University in Prague, Břehová 7, 115 19 Prague, Czech Republic
[3] Faculty of Mathematics and Physics, Charles University, Ke Karlovu 5, 121 16 Prague, Czech Republic

E-mail: davydov@ujf.cas.cz

Received 17 September 2008, in final form 8 January 2009
Published 30 January 2009
Online at stacks.iop.org/JPhysCM/21/095407

Abstract

The present *in situ* neutron diffraction study aims to investigate the response of selected lattice planes in the polycrystalline material upon tensile loading. For this purpose, the 0.1C–0.4Mn construction steel was selected as a simple model material. The tensile deformation test was performed in the incremental mode in which each individual deformation step was followed by unloading. The neutron diffraction spectra were collected both upon loading and unloading and the behavior of the diffraction profiles in the elastic as well as in the plastic region of the deformation curve was examined in detail.

Whereas the behavior of the lattice strains during straining and the evolution of the residual intergranular strains have already been described in other papers, the present work is focused mainly on profile broadening effects measured in the same deformation regime. The estimate of microstrain evolution was done by using the single-line profile analysis method. Comparison of microstrain values in the loaded/unloaded state and in the elastic and plastic regions offers an interesting possibility to estimate the contribution of the *type II* and *type III* microstrains.

(Some figures in this article are in colour only in the electronic version)

1. Introduction

Diffraction methods are valuable experimental tools for the investigation of internal stresses in materials. The neutron diffraction technique has a special position due to the deep penetration depth of thermal neutrons in current materials. This advantage provides a large benefit for stress mapping in bulk components and for *in situ* material testing. The analysis of the position and shape of neutron diffraction profiles can yield valuable information on internal macro- and microstress states in polycrystalline materials. Most neutron diffraction experimental work based on examination of mean lattice spacing (lattice strains) is dedicated to investigation of macrostresses, denoted also as stresses of type I, which is described as the averaged stress for all grains (irrespective of their orientations) in the irradiated volume of the investigated single-phase material. Recently, the resolution of dedicated neutron powder diffractometers has been improved below the limit value $\Delta d/d \approx 2 \times 10^{-3}$ and extraction of other microstructural parameters from neutron diffraction profiles became possible. This method is quite attractive especially due to a chance to characterize the plastically deformed metals *in situ*. Generally, diffraction methods are important when the dislocation density ρ exceeds a critical value of the order of 10^{10} cm^{-2} and direct methods, such as transmission electron microscopy, cannot be applied (Wilkens 1970).

From the point of view of peak profile analysis, two components of line broadening are usually considered: size broadening—the effect of crystallite size, which is independent of the diffraction vector magnitude—and the lattice distortion, i.e. the broadening component which is diffraction-order-dependent and thus increases with the distance from the reciprocal lattice origin. These properties enable the separation of the strain and size effects. Size broadening is caused

by the finite column length of coherently scattering domains where this length is parallel to the diffraction vector (Guinier 1963). Lattice distortions are caused by lattice defects like dislocations, stacking faults, grain boundaries, inclusions, precipitates, etc.

The real structure of plastically deformed crystalline materials has been related to broadened diffraction lines by using various methods of profile analysis. The method of Warren and Averbach (Warren 1957) has been applied by numerous authors (Van Berkum *et al* 1994). Nevertheless, the resulting parameters of that analysis, e.g. the so-called mean square strain $\langle \varepsilon_n^2 \rangle$, are rather difficult to interpret in terms of parameters of the dislocation distribution involved. This new approach has been further adopted for profile analysis, being directly related to the specific properties and arrangement of dislocation lines (Ribárik *et al* 2001). In the present paper, this theoretical approach was introduced to the transformed model fitting/TMF/procedure developed for single-line analysis of neutron diffraction profiles (Strunz *et al* 2001). This modified TMF procedure was used to treat the data from high-resolution neutron diffraction experiments performed on plain ferritic steel *in situ* upon elastic and plastic tensile loading.

The deformation test was performed in the incremental mode in which each individual deformation step was followed by unloading. Comparison of microstrain values in the loaded/unloaded state and in the elastic and plastic regions offer an interesting possibility to estimate the contributions of the type II microstrains, which self-equilibrate over a length scale comparable to that of grain structure, and type III microstrains, self-equilibrated over a length scale which is smaller than the scale of grain structure and includes stresses due to coherence at interfaces and dislocation stress fields.

2. Theoretical overview

2.1. Transformed model fitting/TMF/procedure

The TMF evaluation procedure (Strunz *et al* 2001) based on reciprocal-space modeling and transformed model fitting was developed especially for treatment of single-line neutron diffraction profiles, usually exhibiting larger statistical errors with respect to x-ray diffraction profiles. The proposed TMF method was based on the modeling of experimental data with a Voigt function, i.e. convolution of the Gaussian and the Lorentzian (or Cauchy) curves. The Gaussian function is used for characterization of microstrain in crystalline materials whereas the size contribution is related to the Lorentzian function (de Keijser *et al* 1983, Scardi *et al* 2000). The final modeled profile is obtained by convolution with the instrumental curve of the particular facility. This model is compared with the measured data in an external loop and the optimum parameters are searched for by the least squares method. The TMF procedure permits fast and efficient extraction of simple microstructural parameters from the experimental pattern and is a simple way to study broadened and/or overlapped diffraction profiles (Strunz *et al* 2001). Although the procedure employing broadening models based on a Voigt function reproduce quite well real diffraction data in many cases (Lukáš *et al* 2001), it has certain limits. For example, this procedure does not account for the anisotropy of diffraction line broadening which influences the correctness of the assessed microstructural parameters obtained from a single diffraction line, and can thus be considered as partly legitimate. Moreover, a better microstrain model is available (Wilkens 1970) and is frequently used (Ribárik *et al* 2001, Scardi and Leoni 2002). Similarly, size distribution can be introduced into the broadening effect due to the crystallite size. Therefore, the conventional TMF procedure has recently been extended to more sophisticated broadening models based on the Wilkens dislocation model (Wilkens 1970) and a log-normal grain size distribution (Lloyd 1984, Ribárik *et al* 2001, Scardi and Leoni 2002). This new approach in modeling of the broadening effects in real space provides more realistic microstructure parameters (Van Berkum 1994). Using the Fourier transformation, this model is transformed to the reciprocal space, smeared by instrumental resolution and compared with the measured data.

2.2. Fitting model of single-line diffraction peak broadening

Following the approach used by Warren and Averbach (1950) for multiple reflections, the shape of each diffraction peak can be represented by a Fourier series. The Fourier coefficients of the peak profile, $A(L)$, are the product of the distortion, A^D, and size, A^S, effects (Ungár and Borbély 1996, Ungár and Tichy 1999, Ungár *et al* 2001). If both types of broadening are present, the measured coefficient is the product of the coefficients for each effect:

$$A(L) = A^D(L)A^S(L), \tag{1}$$

where L is the variable of the Fourier transform (Warren and Averbach 1952, Ribárik *et al* 2001). When a single line is measured, distinguishing between the individual contributions can be done on the basis of the profile shape.

The distortion Fourier coefficients A^D can be expressed according to Warren and Averbach (1950)

$$A^D(L) = \exp(-2\pi^2 g^2 L^2 \langle \varepsilon_L^2 \rangle), \tag{2}$$

where g is the absolute value of the diffraction vector, $\langle \varepsilon_L^2 \rangle$ is the mean square strain depending on the displacement of atoms relative to their ideal positions and the angle brackets indicate spatial averaging. Several authors worked on the determination of the mean square strain, assuming either random atomic displacement and/or stacking faults. Later, Krivoglaz (1996) and Wilkens (1970) assumed dislocations as the main source of peak broadening close to the fundamental Bragg positions. The model was improved afterwards by Wilkens by introducing the effective cutoff radius of dislocations R_e^* instead of the crystal diameter. The mean square strain has been derived in the following closed form (Wilkens 1970), assuming infinitely long parallel screw dislocations with a restrictedly random distribution:

$$\langle \varepsilon_L^2 \rangle = (b/2\pi)^2 \pi \rho C f(L/R_e^*), \tag{3}$$

where b is the Burgers vector, ρ is the dislocation density, C is the contrast or orientation factor (Kužel 2007), f is the strain function (the Wilkens function) and R_e^* is the effective

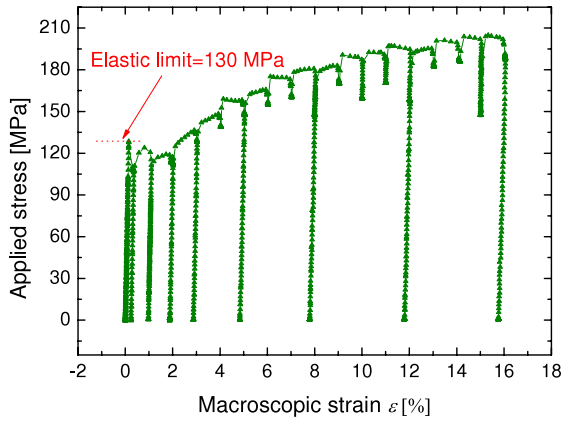

Figure 1. Macroscopic stress/strain response during *in situ* neutron diffraction experiment.

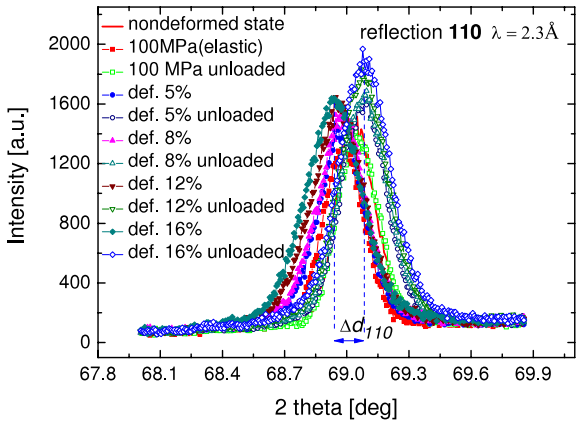

Figure 2. Diffraction peak profiles collected from ferrite {110} reflection at different deformation degrees.

Table 1. Chemical composition of the plain ferritic steel CSN12010/EN10084 (wt%).

C	Si	Mn	P	S
0.100	0.400	0.400	0.035	0.035

outer cutoff radius of dislocations as a second parameter characterizing the dislocation arrangement. The strain function f has an explicit form (Wilkens 1970, in appendix A therein). Strain anisotropy in that model is accounted for by the average contrast factors C of the dislocations, which depend on (i) the indices h, k, l, (ii) on the relative orientations of the line and Burgers' vectors of dislocations and the diffraction vector and (iii) on the elastic constants of the crystal (Ungár *et al* 1999, Ribárik *et al* 2001).

The broadening effect due to the crystallite size can be described in the real space as well. The Fourier transform of the intensity profile of the *hkl* diffraction peak equals the common volume of the crystal and its 'double' obtained by a translation L in the direction normal to the reflecting lattice planes (Ribárik *et al* 2001). For calculation of the Fourier transform of the peak profile originating from a crystallite, according to Guinier (1963) a crystal is considered as divided into cylindrical columns normal to the lattice planes *hkl*. Supposing $\mathrm{d}\sigma_\mu$ as the cross section of the columns, then the heights of these columns in the crystal lie in the interval between μ and $\mu + \mathrm{d}\mu$. The common volume of the irradiated crystallites and their 'double' shifted by L can be obtained by summing for all columns existing in the crystallites. Assuming spherical crystallites and a log-normal crystallite size distribution, the common volume is defined as (Ribárik *et al* 2001)

$$A^s(L) = \int_{|L|}^{\infty} (\mu^2 - |L|\mu)\mathrm{erfc}\left[\frac{\log(\mu/m)}{2^{1/2}\sigma}\right]\mathrm{d}\mu, \qquad (4)$$

where erfc is the complementary error function (Ribárik *et al* 2001), σ is the variance and m is the median of the distribution.

3. Experimental details

The material examined in the present study was 0.1 C–0.4 Mn plain ferritic steel (see table 1) with a yield strength of 130 MPa. The microstructure of this steel consists of relatively large grains with a grain size of about 30 μm. The rod-like specimens of diameter 7 mm and active length 25 mm were prepared for combined diffraction and mechanical testing experiments.

The tensile deformation test was performed in the incremental mode in which each individual deformation step was followed by unloading. The wavelength of the monochromatized beam of cold neutrons used in the experiment was 2.3 Å. The neutron diffraction spectra were collected *in situ* both upon loading (strain-control regime) and unloading and the behavior of the diffraction profiles in the elastic as well as in the plastic region of the deformation curve was examined in detail. The stress–strain curve is shown in figure 1. Neutron diffraction profiles were measured at the dedicated stress/strain diffractometer TKSN-400. Three reflections, 110, 200 and 211, were measured with a relatively high instrumental resolution of $\Delta d/d \sim (2\text{–}2.5) \times 10^{-3}$ at two different orientations of the specimen, axial and radial, i.e. the axis of applied uniaxial stress parallel and perpendicular to the scattering vector, respectively. In such a way, the axial and radial component of the lattice strain tensor was obtained.

Examples of the measured profiles are given in figure 2.

The specimen gauge volume was defined by two slits located in the incident (8 mm) and diffracted beam (4 mm). As input data for the TMF procedure, the instrumental profile and background were measured after each mechanical test. The instrumental profile was approximated by the measured profile from a well-annealed standard specimen of the same dimensions as the tested specimens.

4. Results and discussion

4.1. Behavior of lattice strains

The relative lattice strains are evaluated from the shifts of diffraction peaks during the tensile loading test according to the differentiated Bragg equation (e.g. in Daymond and Priesmeyer 2002, Daymond and Johnson 2001):

$$\varepsilon_{hkl} = \frac{\Delta d_{hkl}}{d_{0,hkl}} = -\cot\theta_{hkl}\,\Delta\theta_{hkl}, \qquad (5)$$

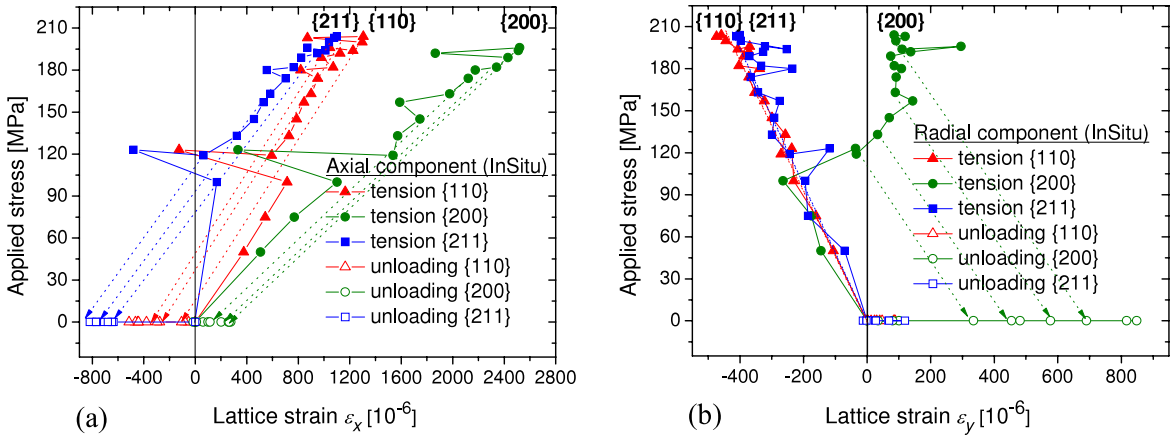

Figure 3. The lattice strain response of different reflection planes in strained specimen parallel (a) and perpendicular (b) to the uniaxial loading.

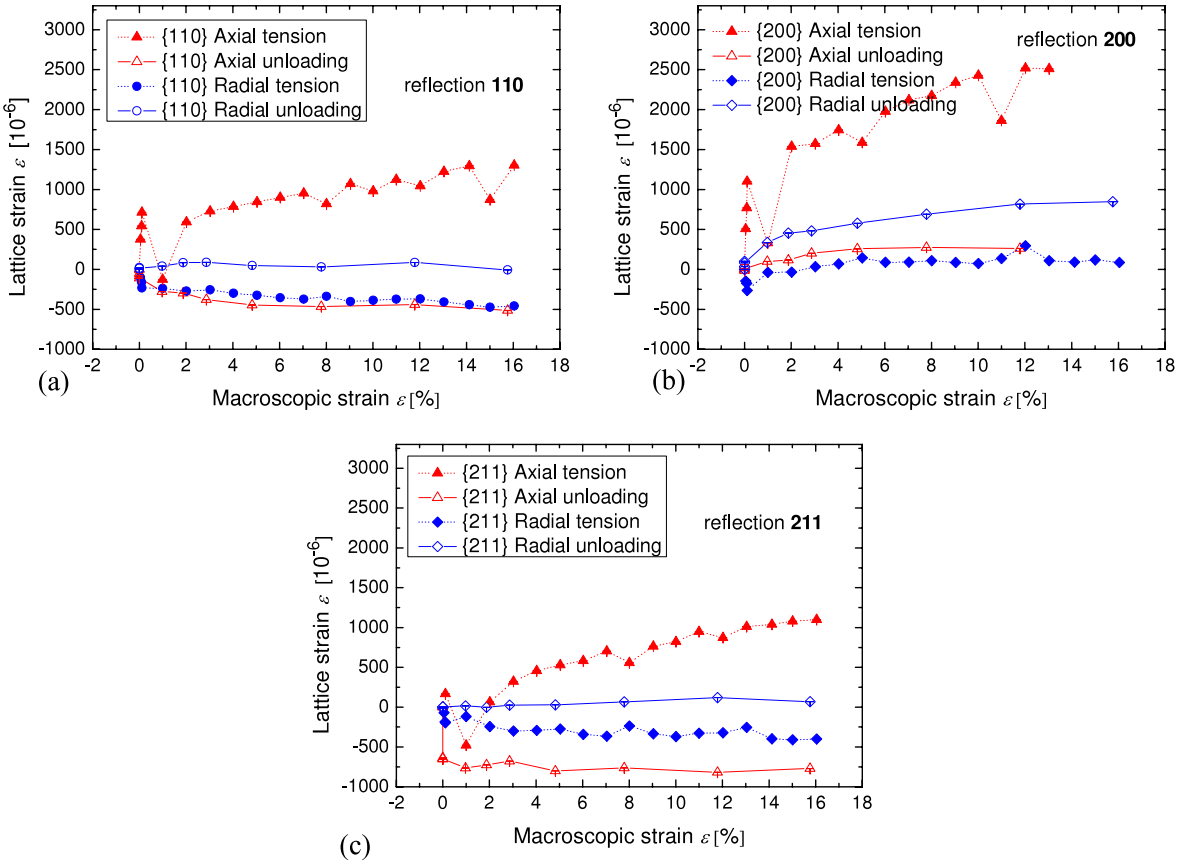

Figure 4. Lattice strain upon tensile straining and relaxation, axial and radial components, reflections 110 (a), 200 (b) and 211 (c). Loaded state is marked by full symbols, unloaded by open symbols.

where θ_{hkl} is the Bragg angle, d_{hkl} is the measured interplanar spacing and $d_{0,hkl}$ is the stress-free interplanar spacing.

The strain determination is then based on measurements of angular deviation of the profile position $\Delta\theta_{hkl}$ from this value related to the stress-free state. In the present case, we consider the interplanar spacing of the virgin state prior to the beginning of the deformation test as the stress-free lattice spacing $d_{0,hkl}$ (figures 3(a) and (b)).

The axial and radial lattice strain components were measured in various loaded states and, following relaxation, the individual measuring points can be seen in the stress–strain curve in figure 1. The observed lattice strain curves from examined reflections show different behavior (see figure 4).

The behavior of 110 and 211 lattice strains during elastic straining is similar in every crystallite with the corresponding orientation to the loading axis; these lattice planes are referred to as stiff crystallographic directions due to their elastic anisotropic properties. When plastic deformation starts, the behavior of lattice planes also becomes affected by the plastic anisotropy, defined by the different plastic deformation of

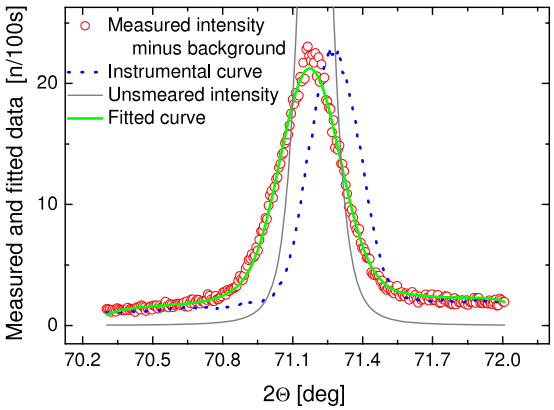

Figure 5. Refinement of the 110 diffraction profile by modified TMF procedure. Data collected upon 12% of tensile deformation. Unsmeared intensity represents the modeled intensity curve without instrumental broadening.

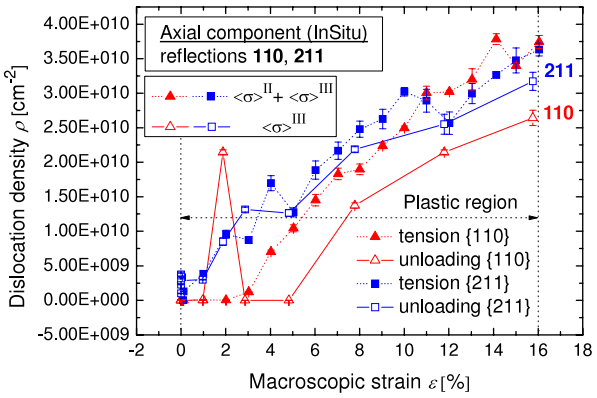

Figure 6. Evolution of dislocation densities upon tensile straining and relaxation, extracted from the analysis of 110 and 211 profiles.

neighboring grains according to their orientations with respect to the load axis. These elastic and plastic anisotropic properties are responsible for the unique behavior of {200} lattice planes, which are the most compliant in the cubic symmetry, and reach the relaxed state upon unloading in the axial direction and loading in the radial direction (figure 4(b)). Here the maximum level of lattice strains ε_{110} and ε_{211} upon loading is considerably lower than in the case of ε_{200}.

Moreover, the evolution of residual lattice ε_{200} strains in radial and axial directions observed after unloading from different deformation degrees indicate a strong influence of the intergranular strains caused by the intergranular grain shape misfits generated by differential slipping during deformation (Hutchings *et al* 2005 p 242). In general, intergranular stresses generated during loading have two origins; elastic anisotropy due to directional variation of the elastic properties of the single crystal and plastic anisotropy due to the preferential deformation in slip planes and slip directions.

4.2. Microstructural parameters

The modified TMF evaluation method described in section 2 was employed for profile analysis of the observed diffraction lines. Due to large grain size, the size effect has been found to be negligible and the profile broadening can be treated in terms of the dislocation model only. Even at the high level of plastic deformation the grain size is still large and its contribution is possible to neglect, considering merely the contribution from microstrains in the refinement procedure. To obtain physically correct microstructural parameters, knowledge of the averaged contrast factor is obviously of essential importance. The calculation of contrast factors was performed by the program ANIZC[4] (Borbély *et al* 2002) based on the method of Teodosiu (1982), with further averaging over all symmetrically equivalent directions of crystal symmetry. According to the body-centered cubic structure of the studied steel the edge {110}⟨111⟩ and screw ⟨111⟩ types of dislocations were chosen as the common slip planes and directions. The ratio of the types of dislocations has been assessed on the basis of calculated average contrast factors for the reflections used and equals 47% for edge and 53% for screw type (Borbély *et al* 2000).

Figure 5 shows the outcome of the procedure of refinement of the 110 diffraction peak from the ferrite phase, performed for the whole set of diffraction data collected at every deformation step. Results of analysis of 110 and 211 profiles are displayed in figure 6. The analysis of the 200 reflection did not yield reliable results due to the insufficient statistics of the measured profiles, resulting in large errors in fitted values of microstructural parameters. The dislocation densities resulting from the fitting procedure for 110 and 211 reflections show very close values and similar evolution with macroscopic deformation. It indicates reasonable input values of the contrast factors having an influence on the scaling factor. A similar parabolic dependence of the evolution of dislocation density—but with higher values—was presented in the work of Scardi and Leoni (2002). In that case, the ball-milled Ni powder samples were investigated *ex situ*, which made possible only the evaluation of relaxed states of severely deformed material.

Comparison of dislocation density curves in the loaded and relaxed state in figure 6 shows the very interesting effect of reversible changes of microstrain represented by the dislocation density (Tomota *et al* 2003). This effect is caused most probably by the different behavior of contributions of microstrains' type II and type III. The nature of the observed reversible changes of dislocation densities can be explained by the mixed microstrains of type II and type III in the case of straining, and by the microstrain of type III in the relaxed state. The latter is ascribed to the pure dislocation density. The proposed interpretation is plotted in figure 7. separately for 110 reflections where this effect is strongly pronounced. The pure reversible component of microstrain is assumed to be represented by the heterogeneous elastic strain of type II (Davydov *et al* 2008). Although it is known that the source of type II stresses is not due to dislocations, their representation in figures 6 and 7 together with type III stresses have a purpose merely to simplify the comprehension of the proposed theory of diverse types of stress separation.

[4] The ANIZC program is available *via* the World Wide Web and can be found at the homepage of the Department of General Physics, Eötvös University, Budapest (http://metal.elte.hu/anizc).

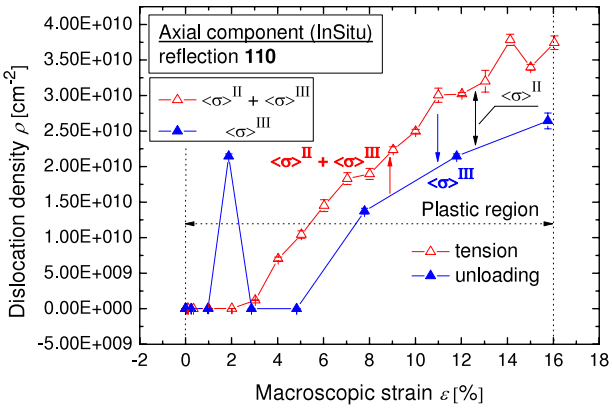

Figure 7. Proposed interpretation of reversible changes in profile broadening.

The anomalous dislocation density value at 2% of macroscopic strain in the relaxed curve of the 110 reflection seems to be incorrect. Nevertheless, similar deviations appear systematically in all measured radial and axial directions for this particular reflection and could thus be considered as real. This anomalous increase of microstrain at $\varepsilon = 2\%$ macroscopic strain follows an anomalous relaxation of elastic lattice strain in the previous deformation step $\varepsilon = 1\%$ (see figures 3(a) and (b)). This effect can be possibly associated with the phenomenon of the Lüders band. Following the proposed interpretation and for a better insight into heterogeneous elastic strain type II, the dislocation density in the relaxed state was extrapolated for each measuring step. This dependence was used as a fixed input function of dislocation density in the fitting procedure and all profiles were fitted again with the assumption of such a dislocation density. The additional broadening of profiles was treated in the form of a Gaussian distribution of the corresponding lattice parameter.

The difference between extrapolated values of dislocation density upon unloading and the values when the load was applied represents the heterogeneous elastic strain of type II. This strain can be represented by a relative value of width of the fitted d-spacing distribution or, more illustratively, as the root mean square strain (RMSS) of the Warren and Averbach model (Warren and Averbach 1950, de Keijser *et al* 1983).

The estimated magnitudes of elastic strain of type II in terms of RMSS versus macroscopic strain and applied stresses are presented in figure 8. In the plastic region of deformation, the values follow roughly a parabolic dependence (figure 8(a)), similarly to the evolution of dislocation densities (figure 7).

The observed values of heterogeneous type II strain in the elastic area are almost negligible, although such an effect is, in principle, possible due to elastic anisotropy and a significant linear dependence had been observed in the case of other examined high-strength steels (Muránsky 2006).

The present incremental deformation experiment yields various information on the evolution of internal strains. The centers of the diffraction profiles and their reverted shifts are interpreted in terms of the average level of elastic lattice strains (type II) whereas profile broadening has been interpreted as a reversible heterogeneous elastic strain type II and irreversible microstrain type III due to dislocations. The heterogeneous elastic strains (figure 8) correspond to the mean deviation of the lattice strains from the averaged values (figure 4). The evolution of lattice strains shown in figures 4(a)–(c) is influenced by elastic and plastic anisotropy and the contribution of the elastic anisotropy can be estimated from figure 8. This assumption is not exactly correct because the stress state of the material upon relaxed external stress is influenced not only by the microstrain of type III but also by the residual strain of type II (Hutchings *et al* 2005 p 12). However, the present experiment does not allow us to distinguish this residual strain type II contribution.

5. Conclusions

During mechanical tensile tests performed *in situ* at the high-resolution neutron diffractometer, the reversible changes in neutron diffraction line broadening were observed upon tensile straining and subsequent relaxation. The reversible changes in peak width are supposed to be caused by the heterogeneous elastic strain distribution between particular grain families

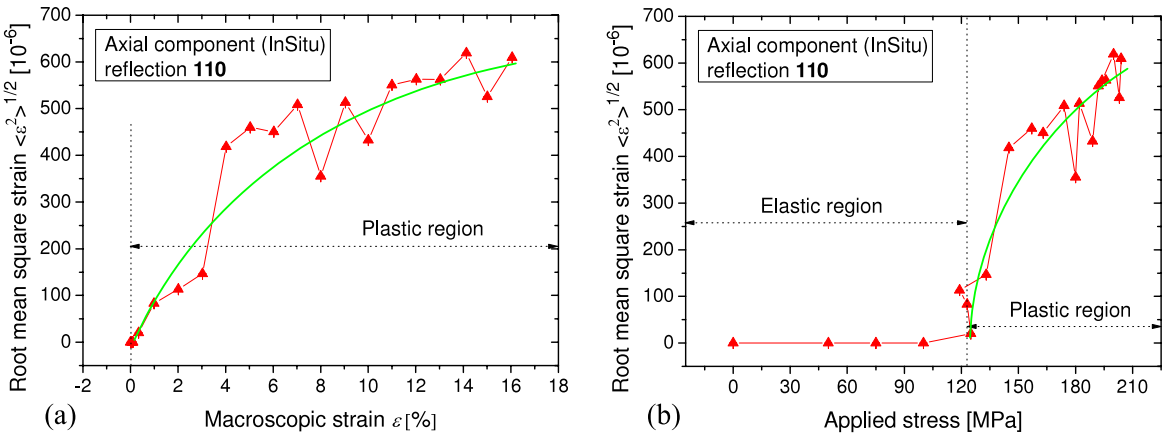

Figure 8. Fitted evolution of the elastic microstrain type II as a function of macroscopic strain (a) and applied stress (b).

within the strained sample. The proposed interpretation of reversible effects is based on the assumption that diffraction line broadening observed upon loading corresponds to the total microstress of type II and type III, where type II consists of two subtypes, residual (Hutchings *et al* 2005 p 12) and heterogeneous elastic components. The broadening in the relaxed state pertains to a quantity of dislocation density and is caused preferentially by type III plus a residual component of type II stresses.

The modified and extended procedure of the single-line diffraction profile analysis based on Wilkens' dislocation model and the log-normal size distribution was reviewed and tested in the study of plain ferritic steel. This new procedure seems to be an effective tool in the determination of dislocation densities and could be applied for a set of diffraction profiles as well, using the appropriate contrast (orientation) factors.

Acknowledgments

The authors are grateful to the Grant Agency of the ASCR (contract IAA100480704) and Ministry of Education of Czech Republic (MSMT 2486 G1) for supporting this research. The first author is also grateful to the NMI3 project (FP6-RII3-CT-2003-505925), ISIS and Lund University for the partial financial support for participation in the 4th ECNS. One of the authors (R Kužel) gratefully acknowledges support by grant MSM 0021620834.

References

Borbély A, Blum W and Ungár T 2000 On the relaxation of the long-range internal stresses of deformed copper upon unloading *Mater. Sci. Eng.* **A276** 186–94

Borbély A, Dragomir J, Ribárik G and Ungár T 2002 Computer program ANIZC for the calculation of diffraction contrast factors of dislocations in elastically anisotropic cubic, hexagonal and trigonal crystals *J. Appl. Crystallogr.* **36** 160–2

Davydov V, Lukáš P, Strunz P and Kužel R 2008 Single-line diffraction profile analysis method used for evaluation of microstructural parameters in the plain ferritic steel upon tensile straining *Mater. Sci. Forum* **571/572** 181–8

Daymond M R and Johnson M W 2001 The determination of a stress-free lattice parameter within a stressed material using elastic anisotropy *J. Appl. Crystallogr.* **34** 263–70

Daymond M R and Priesmeyer H G 2002 Elastoplastic deformation of ferritic steel and cementite studied by neutron diffraction *Acta Mater.* **50** 1613–26

de Keijser Th H, Mittemeijer E J and Rozendaal C E 1983 Use of the Voigt function in a single-line method for the analysis of x-ray diffraction line broadening *J. Appl. Crystallogr.* **16** 309–16

Guinier A 1963 *X-Ray Diffraction* (San Francisco, CA: Freeman)

Hutchings M T, Withers P J, Holden T M and Lorentzen T 2005 *Introduction to the Characterization of the Residual Stress by Neutron Diffraction* (Boca Raton, FL: Taylor & Francis)

Krivoglaz M A 1996 *X-ray and Neutron Diffraction in Nonideal Crystals* (Berlin: Springer)

Kužel R 2007 Kinematical diffraction by distorted crystals—dislocation x-ray line broadening *Z. Kristallogr.* **222** 136–49

Lloyd E 1984 *Handbook of Applicable Mathematics* vol 4 *Statistics* (Chichester: Wiley)

Lukáš P, Novák V, Šittner P and Neov D 2001 *In situ* high resolution neutron diffraction study of anisotropy and stress effects in transforming CuAlZnMn shape memory alloys *J. Neutron Res.* **9** 79–86

Lukáš P, Tomota Y, Harjo S, Neov D, Strunz P and Mikula P 2001 *In situ* neutron diffraction study of drawn pearlitic steel wires upon tensile deformation *J. Neutron Res.* **9** 415–21

Muránsky O 2006 *In situ* neutron diffraction studies of deformation and transformation processes in modern types of steels *PhD Thesis* Charles University, Prague

Ribárik G, Ungár T and Gubicza J 2001 MWP-fit: a program for multiple whole profile fitting of diffraction peak profiles by *ab initio* theoretical functions *J. Appl. Crystallogr.* **34** 669–76

Scardi P and Leoni M 2002 Whole powder pattern modelling *Acta Crystallogr.* A **58** 190–200

Scardi P, Leoni M and Delhez R 1999 Fourier modelling of the anisotropic line broadening of x-ray diffraction profiles due to line and plane lattice defects *J. Appl. Crystallogr.* **32** 671–82

Scardi P, Leoni M and Dong Y H 2000 Whole diffraction pattern-fitting of polycrystalline fcc materials based on microstructure *Eur. Phys. J.* B **18** 23–30

Strunz P, Lukas P and Neov D 2001 Data evaluation procedure for high-resolution neutron diffraction methods *J. Neutr. Res.* **9** 99–106

Teodosiu C 1982 *Elastic Models of Crystal Defects* (Berlin: Springer)

Tomota Y, Lukáš P, Neov D, Harjo S and Abe Y R 2003 *In situ* diffraction during tensile deformation of a ferrite–cementite steel *Acta Mater.* **51** 805–17

Ungár T and Borbély A 1996 The effect of dislocation contrast on x-ray line broadening: a new approach to line profile analysis *Appl. Phys. Lett.* **69** 3173–5

Ungár T, Dragomir I and Révész A 1999 Borbély: the contrast factors of dislocations in cubic crystals: the dislocation model of strain anisotropy in practice *J. Appl. Crystallogr.* **32** 992–1002

Ungár T, Gubicza J, Ribárik G and Borbély A 2001 Crystallite size distribution and dislocation structure determined by diffraction profile analysis: principles and practical application to cubic and hexagonal crystals *J. Appl. Crystallogr.* **34** 298–310

Ungár T and Tichy G 1999 The effect of dislocation contrast on x-ray line profiles in untextured polycrystals *Phys. Status Solidi* a **171** 425–34

Van Berkum J G M 1994 Strain fields in crystalline materials. Methods of analysis based on x-ray diffraction-line broadening *PhD Thesis* Delft University of Technology, The Netherlands

Van Berkum J G M, Vermuelen A C, Delhez R, de Keijser T H and Mittemeijer E J 1994 Applicabilities of the Warren–Averbach analysis and an alternative analysis for separation of size and strain broadening *J. Appl. Crystallogr.* **27** 345–57

Warren B E 1957 X-ray studies of deformed metals *Prog. Met. Phys.* **8** 147

Warren B E and Averbach B L 1950 The effect of cold-work distortion on x-ray patterns *J. Appl. Phys.* **21** 595

Warren B E and Averbach B L 1952 The separation of cold-work distortion and particle size broading in x-ray patterns *J. Appl. Phys.* **23** 497

Wilkens M 1970 The determination of density and distribution of dislocations in deformed single crystals from broadened x-ray diffraction profiles *Phys. Status Solidi* a **2** 359–70